Thermoelectric generation using counter-flows of ideal fluids

Xiangning Meng [1, 3], **Baiyi Lu** [1], **Miaoyong Zhu** [1], **Ryosuke O. Suzuki** [2]

1. School of Metallurgy, Northeastern University, Shenyang 110819, China

2. Faculty of Engineering, Hokkaido University, Sapporo 060-8628, Japan

3. e-mail: mengxn@smm.neu.edu.cn

Abstract: Thermoelectric (TE) performance of a three-dimensional (3D) TE module is examined by exposing it between a pair of counter-flows of ideal fluids. The ideal fluids as thermal sources of TE module flow in the opposite direction at same flow rate and generate temperature difference on the hot and cold surfaces due to their different temperature at channel inlet. TE performance caused by different inlet temperature of thermal fluids are numerically analyzed by using finite-volume method on 3D meshed physical models and then compared with those of using constant boundary temperature. The results show that voltage and current of TE module increase gradually from a beginning moment to a steady flow and reach a stable value. The stable values increase with inlet temperature of hot fluid when inlet temperature of cold fluid is fixed. However, the time to get the stable values is almost consistent for all the temperature differences. Moreover, the trend of TE performance using fluid flow boundary is similar to that of using constant boundary temperature. Further, 3D contours of fluid pressure, temperature, enthalpy, electromotive force, current density and heat flux are exhibited in order to clarify the influence of counter-flows of ideal fluids on TE generation. The current density and heat flux homogeneously distribute on entire TE module, thus indicating that the counter-flows of thermal fluids have high potential to bring fine performance for TE module.

Key words: Thermoelectric generation, Thermoelectric device, Fluid flow boundary, Counter-flows, Heat transfer, Finite-element analysis

1. Introduction

Thermoelectric (TE) conversion is a method of directly converting the heat into electricity, which is based on the Seebeck effect at a junction of two different materials, and has many practical advantages in terms of access to energy [1, 2]. TE generator can be operated reliably in an isolated place without noise and pollution to harvest inexhaustible resources and low-grade energy, such as renewable solar heat and unrecovered waste heat, and chemical reactions or mechanical moving parts are no longer needed [3, 4]. A premise of TE conversion is that a temperature difference exists between hot and cold surfaces of TE module. Thermal sources which cause the temperature difference can be presented in various forms. Our previous works discussed the basic TE phenomenon under constant thermal conditions for various module designs, *i.e*. fixed the temperature or the heat flux on hot and cold surfaces and analyzed TE performance of the helical and conventional straight panels, as well as modules consisting of tilted parallelogram- and polyhedron-shaped thermo-elements [5-9]. However, the most likely approach to utilize the residual heat of waste fluids is to allow the high-temperature gas and liquid to flow on module surfaces. This study conducted fluid dynamics simulations using finite-volume method on a three-dimensional (3D) meshed physical models in a commercial software environment, FLUENT, to illustrate TE generation from a beginning moment of fluid flow to a steady flow on a conventional straight TE module, which exposed between a pair of counter-flows of ideal fluids, and then to call a trigger for investigating the influence of thermal fluid flow on TE conversion. Here, we temporarily ignored the temperature-dependent properties of ideal fluid in order to simplify the calculation, and the ideal fluid is considered to be a thermal source with a given initial temperature and flow at a set flow rate.

2. Modeling

2.1 Finite-Element Entity Models

A conventional TE module is meshed in order to numerically conduct finite-element simulations for TE generation analysis, as depicted in **Figure 1**, where rectangular elements of p-type and n-type are connected together in series. TE conversion is induced by the temperature difference between hot and cold surfaces. The thermal conditions applied to TE module can be scattered boundary as shown in **Figure 1 (a)**, can also be flow boundary as shown **Figure 1 (b)**, or a combination of both. The scattered thermal boundary is mostly caused by the homogeneously distributed heat sources, such as thermal radiation and solar heat, as well as directional heat-conduction of solid contact. The fluid flow boundary can only be attributed to the carrying heat of thermal fluids, containing gas and liquid with different temperature.

Further, we regarded the hot and cold surfaces as floors to construct two channels for thermal fluid flow on both sides of TE module, as shown in **Figure 2**, where also contains two walls and a ceiling. This 3D design allows a pair of counter-flows of hot and cold fluids flow into the channels via the inlet, and flow out of the channels via the outlet, respectively, and leads to a heat harvesting for TE conversion on TE module. In this study, we let the hot and cold fluids flow into channel inlet at a fixed flow rate, and then to examine the characteristic performances of TE module by using 3D finite-element analysis. Transient performances caused by the fluids with different temperature are calculated from a beginning moment of fluid flow to a steady flow, and the change trend of stable values of these characteristic performances are compared with those of using a scattered thermal boundary, *i.e.* fixed a constant temperature on the hot and cold surfaces.

For simplification, we made the following assumptions: (1) TE module is adiabatic to the outside, (2) perfect tight bonding exists among all the component parts, (3) temperature-dependent properties of all materials are ignored, (4) no change in pressure and volume for ideal fluids, and the hot and cold fluids are considered as oil and water, respectively, and (5) ideal fluids present a steady laminar flow in one-way, and the fluid compression and the turbulent buoyancy in channel are neglected. Moreover, we assumed that the physical properties of

high-temperature oil are close to those of water at ambient temperature, so that ensure the one-way flow and the heat transfer of hot and cold fluids are in a similar situation. The properties of the materials and the geometric dimensions of 3D physical model are listed in **Table 1**, **Table 2** and **Table 3**, respectively. Here the issue of obtaining a high TE performance by matching the geometric parameters and the physical properties of p-type and n-type elements is temporarily ignored.

2.2 Governing Equations

The laminar flow of ideal fluids follows the law of mass conservation, and the continuity equation is expressed as:

$$\nabla \cdot v = \frac{\partial v_x}{\partial x} = 0 \tag{1}$$

where the flow rate of ideal fluids is: $v = v_x + v_y + v_z$, and only a flow rate, v_x, which is in the direction of one-way flow, is available for the incompressible fluids. Based on the law of momentum conservation, the motion equation of ideal fluids is represented by the Euler equation [11]:

$$f - \frac{1}{\rho_F}\nabla p = \frac{\partial v_x}{\partial t} \tag{2}$$

where ρ_F is the density of ideal fluids, f is the mass force caused by the gravity, and p is pressure in fluids.

Heat of ideal fluids is applied to the hot and cold surfaces as thermal inputs, and thus results in TE conversion, as well as the heat flux and the electromotive force. Heat conduction of TE module is given by **Eq. 3**. The left side represents the heat transfer that follows the Fourier law, and the right side includes two terms: the Joule heat

generated by the current, and the heating or cooling caused by the Thomson effect.

$$\nabla \cdot (\lambda \Delta T) = T\boldsymbol{J} \cdot \nabla S - \rho |\boldsymbol{J}|^2 \tag{3}$$

where λ, ρ, and S denote the thermal conductivity, the electric resistivity, and the relative Seebeck coefficient, respectively, and the current density, $\boldsymbol{J}$, is obtained by the electric potential and the temperature using **Eq. 4**.

$$\rho\boldsymbol{J} = -\nabla V - S\nabla T \tag{4}$$

where the voltage due to $\rho\boldsymbol{J}$ is expressed by the change in the electric potential, ∇V, and the voltage generated from the Seebeck effect, $S\nabla T$. Further, a governing equation, **Eq. 5**, can be derived from **Eq. 4** by applying electric charge conservation.

$$\nabla \cdot (\nabla V + S\nabla T) = 0 \tag{5}$$

We used **Eq. 1** and **Eq. 2** to define the flow state of ideal fluid, and conducted the numerical simulations by solving the simultaneous differential equations of **Eq. 3** and **Eq. 5** based on the finite-volume method in the commercial software package, FLUENT, and then to determine the characteristic performances of TE module in a 3D physical model, which using a fluid flow boundary. By referring to the reported codes [12, 13], our custom-written C program is embedded into FLUENT and combined with conventional codes to evaluate the current density [14, 15].

3. Results and Discussion

3.1 Transient Performance

This study set the inlet temperature of hot fluid as 400 K, 450 K, 500 K, 550 K, and 600K, and that of cold fluid is 300 K, respectively. Two fluids incessantly flow in the opposite direction at a constant flow rate of 5.0 $mm \cdot s^{-1}$. TE module consists of 18 pairs of p-type and n-type elements, *i.e.* p-n pairs, and the fluid channel length is calculated as 53.5 mm according to the geometric dimensions of 3D physical model. The time of fluid flowing through the entire channel can be theoretically calculated as 10.7 s. So, we conducted the numerical simulations in a period of 25.0 s from a beginning moment to a steady flow of fluid in order to ensure the sufficient time to obtain stable values of performance.

Transient characteristic performances calculated by using fluid flow boundary are shown in **Figure 3**. We can observe an interesting phenomenon that the direction of voltage and current generated in the initial stage of fluid flow, approximately 1.0 s, is reversed to that of subsequent voltage and current. This is because p-n pairs near the channel inlets generate the electromotive force and the electric current on TE module based on the Seebeck effect, which caused by the local temperature difference, but the others p-n pairs consume the electric current to form a reverse temperature gradient based on the Peltier effect, and then produce the short-lived electromotive force and electric current in a reversed direction. Since then, the voltage and current gradually start to increase with the fluid flow. The performance failed to achieve a stable value in the theoretical time of 10.7 s that the hot and cold surfaces are completely covered by the thermal fluids, but is delayed for about 6.0 s and get stable values at time of 17.0 s. Higher inlet temperature of hot fluid results in larger temperature difference between hot and cold surfaces, so that the stable values of voltage and current are increased correspondingly because the electromotive force of TE module is the sum of the multiplication of the relative Seebeck coefficient and the temperature difference for all elements connected in serial. The increments of stable voltage and current are

linearly increased with the inlet temperature of hot fluid, and they are approximately 0.79 mV and 3.37 mA for each temperature increase of 50 K, respectively. Similarly, the output power of TE module is also gradually increased and reached a stable value after a small fluctuation in the initial stage. Higher inlet temperature of hot fluid also leads to larger increment of output power, 13.32 mW and 29.35 mW, when the inlet temperature increased from 400 K to 450 K and from 550 K to 600 K, respectively. Further, the stable performance values of TE module are listed in **Table 4**, and the change trend of them can be understood.

This study compared the stable values of characteristic performances with those of using constant boundary temperature by referring to the previous results [9], which obtained by sequentially varying the constant temperature of hot surface to 400 K, 450 K, 500 K, 550 K and 600 K, so as to produce the temperature difference of 100 K, 150 K, 200 K, 250 K and 300 K between hot and cold surfaces by fixed the temperature of cold surface at 300 K. The voltage and current calculated by using fluid flow boundary and constant boundary temperature, respectively, are shown in **Figure 4 (a)** and **(b)**. The voltage and current present linear increase with the inlet temperature of hot fluid and the temperature difference for two boundary conditions, and their change trends are consistent. Thus, it can be known that the steady flow of thermal fluids also causes a stable thermal boundary for TE module to generate stable performance, and exactly similar to that done by the constant boundary temperature. The change trends of output power for two boundary conditions are identical because they are obtained by multiplying voltage and current, and then present a parabolic curve, as illustrated in **Figure 5 (a)** and **(b)**. Moreover, the input heat absorbed by the hot surface of TE module is calculated by extracting the heat flux of all surface meshes and multiplying them with their area. The sums of these products are given in **Figure 5 (c)** and **(d)**. The stable thermal boundary caused by the steady flow of fluids brings a relatively fixed heat supply from the hot fluid, and the input heat is linearly increase with the inlet temperature of hot fluid and temperature difference for two boundary conditions. The conversion efficiency of TE module is defined by the

ratio of the output power to the input heat absorbed at hot surface and **Figure 6** provided the efficiencies of using two boundary conditions, which determined by the results in **Figure 5**. The conversion efficiencies for two conditions have the similar change trend that they all linearly increase with the inlet temperature of hot fluid and temperature difference. However, the conversion efficiency obtained by using fluid flow boundary is significantly lower than that of using constant boundary temperature. We consider that the suitable fluid flow boundary depends simultaneously on the flow rate and mass of thermal fluids, as well as the geometric dimensions of fluid channel, and the modest study on the utilization of fluid flow boundary for TE generation will be conducted separately.

3.2 Module Features

3D contours of TE module, including steady fluid pressure, temperature, enthalpy, electromotive force, current density and heat flux are exhibited in order to present the module features of employing the counter-flows of ideal fluids as the fluid flow boundary for TE generation, and then to reveal the influence of counter-flows on TE performance.

The pressure of steady flow of thermal fluids in channel is shown in **Figure 7**. The pressure distributions of hot and cold fluids are consistent for the different inlet temperature of hot fluid, and the pressure values are also same because the temperature-dependent properties of ideal fluids are ignored in this study. The pressure in channel is static pressure of fluids, and thus it is only significantly affected by the geometric configuration of TE module, and the pressure of hot fluid is higher than that of cold fluid due to their own gravity. The maximum pressure 470.0 Pa appears at channel inlet of hot fluid and then gradually decreases to be 282.0 Pa at channel outlet, and the pressure of cold fluid naturally drops from 183.0 Pa at channel inlet to 0 at channel outlet of cold fluid.

The temperature over the entire TE module is depicted in **Figure 8**. The distribution trend of temperature are consistent for the different inlet temperatures of hot fluid, 400 K, 450 K, 500 K, 550 K, and 600 K, and the fixed inlet temperature of cold fluid, 300 K. The hot fluid is cooled and the cold fluid is heated at the same time by exchanging heat through the conduction of solid module, so as to beneficially generate a homogeneous temperature difference between the hot and cold surfaces of TE module, which has become an advantage of harvesting heat of thermal fluids to achieve TE generation by using a pair of counter-flows, as illustrated by sub-graph of **Figure 8**.

The specific enthalpy of TE module in a steady state is presented in **Figure 9**. Higher inlet temperature of hot fluid leads to more energy changes, and the highest enthalpy appears at the channel inlet of hot fluid with high-temperature and then gradually reduces toward the channel inlet of cold fluid. The maximum enthalpy of TE module is linearly increased with inlet temperature of hot fluid from 427.8 $MJ \cdot kg^{-1}$ with temperature 400 K to 1267.8 $MJ \cdot kg^{-1}$ with temperature 600 K. However, the minimum enthalpy is no longer rising after the inlet temperature of hot fluid reaches a temperature of 500 K, which because the inlet temperature of cold fluid is fixed at 300 K and the sustaining increase of internal energy of ideal fluids is restricted.

The steady electromotive force on TE module is given in **Figure 10**. The electromotive force is generated only on the conductive p-n pairs and the electrode plates. The maximum electromotive force is linearly increased with inlet temperature because it is the sum of the multiplication of the relative Seebeck coefficient and the temperature difference of TE elements for all serial connections.

A p-n pair is enlarged in **Figure 11** to reveal the distribution trend of current density on TE module. The linear growth of electromotive force results in a linear increase of electric current as TE module is connected with external resistance to form a closed electric circuit. The current density also increases linearly in an unchanged module body. The electric charges homogeneously distribute on p-type and n-type elements because of their

large volume, and there is no obvious low-density area on TE elements, and thus it indicates that the counter-flows of hot and cold fluids can produce uniform current density on the conventional cube elements. The maximum current density appears at the central region of the electrode plate, as pointed by the black arrows in **Figure 11**, because it is a narrow path for the current flow. The maximum density linearly increases with inlet temperature of hot fluid from 68.1 $kA \cdot m^{-2}$ at 300 K to 200 $kA \cdot m^{-2}$ at 600 K.

The distribution of heat flux is displayed in **Figure 12**. The heat flux presents different values in different locations of TE module because its distribution largely depends on the geometric configuration of module and is affected by the materials properties. For example, a part of heat is gathered and flows into the corner of the electrode plates, as depicted by the red arrows in **Figure 12**, because the insulator layer is not completely in contact with the electrode plate when the heat of thermal fluids is transferred through the sandwiched electrode plate from insulator layer to p-type and n-type elements, and these heat can only be conducted in this way. Naturally, more heat leads to a larger heat flux in the corresponding regions, as delineated by the rhomboid blocks in **Figure 12**. However, the heat flux on the entire module still represents a relatively uniform trend. This means that the counter-flows of thermal fluids have a promising potential to generate fine TE performance because the homogeneous diffusivity of heat is essential for a high-quality TE module.

3. Conclusions

Performance of a TE module using the ideal fluids of ignoring temperature-dependent properties as the thermal fluids is examined in order to call a trigger to study the influence of counter-flows of hot and cold fluids on TE conversion. The results are drawn as follows:

(1) TE performance tends to be stable over a period of time after the module surfaces are completely covered by the thermal fluids. The delay time is consistent for the different inlet temperature of hot fluid when the

inlet temperature of cold fluid and the flow rate of counter-flows are fixed. Stable performance values increase with inlet temperature of hot fluid, which is similar to those of with constant boundary temperature.

(2) Steady counter-flows of thermal fluids can provide a favorable thermal boundary on TE module by generating a homogeneous temperature difference between hot and cold surfaces. Fluid flow boundary using counter-flows is advantageous for harvesting the heat from thermal fluids to achieve TE generation.

(3) Electric charges homogeneously distribute on conventional cube elements of p-type and n-type as the fluid flow boundary is used. Heat flux also uniformly conducted on TE module. Hence, counter-flows of thermal fluids have a promising potential to generate fine performance for TE conversion.

Acknowledgements

The authors are grateful to financial supports from National Natural Science Foundation of China (51576034) and Research Grant-in-Aid of JSPS (26630490).

References

1. K. V. Selvan and M. S. M. Ali. *Renew*. *Sust*. *Energ*. *Rev*. 54, 1035 (2016).

2. D. V. Singh and E. Pedersen. *Energ*. *Convers*. *Manage*. 111, 315 (2016)

3. G. J. Snyder and E. S. Toberer. *Nat*. *Mater*. 7, 105 (2008).

4. A. Dewan, S. U. Ay, M. N. Karim, and H. Beyenal. *J. Power Sources* 245, 129 (2014).

5. X. Meng and R. O. Suzuki. *Appl. Therm. Eng*. 99, 352 (2016).

6. R. O. Suzuki, K. O. Ito, and S. Oki. *J. Electron. Mater.* 45, 1827 (2016).

7. R. O. Suzuki, T. Fujisaka, K. O. Ito, X. Meng, and H. Sui. *J. Electron. Mater.* 44, 348 (2015).

8. X. Meng and R. O. Suzuki. *J. Electron. Mater.* 44, 1469 (2015).

9. X. Meng, T. Fujisaka, and R. O. Suzuki. *J. Electron. Mater.* 43, 1509 (2014).

10. D. M. Rowe. *CRC Handbook of Thermoelectrics*, (Florida: CRC Press, 1995), p. 445.

11. X. Z. Zhang. *Principles of Transfer in Metallurgy*, (Beijing: Metallurgical Industry Press, 2005), p. 42.

12. M. Chen, L.A. Rosendahl, and T. Condra, *Int. J. Heat Mass Transf.* 54, 345 (2011).

13. A. Rezania and L.A. Rosendahl. *J. Electron. Mater.* 41, 1343 (2012).

14. T. Fujisaka, H. Sui, and R. O. Suzuki. *J. Electron. Mater.* 42, 1688 (2013).

15. X. Meng and R. O. Suzuki. *Mater*. *Trans*. 56, 1092 (2015).

Figure captions

Figure 1 Thermal boundary conditions of a TE module: **(a)** scattered thermal boundary and **(b)** fluid flow boundary.

Figure 2 3D design of a TE module using fluid flow boundary.

Figure 3 Transient characteristic performances of TE module.

Figure 4 Voltage and current using different boundary conditions.

Figure 5 Output power using **(a)** constant temperature boundary and **(b)** fluid flow boundary as well as corresponding input heat **(c)** and **(d)**.

Figure 6 Conversion efficiency using **(a)** constant boundary temperature and **(b)** fluid flow boundary.

Figure 7 Pressure of thermal fluids in channel.

Figure 8 Temperature distribution of TE module.

Figure 9 Specific enthalpy of TE generation.

Figure 10 Electromotive force of TE module.

Figure 11 Current density of TE module.

Figure 12 Heat flux on TE module.

Table captions

Table 1 Thermal and electric properties of materials [9, 10].

Table 2 Physical properties of water at ambient temperature.

Table 3 Geometric dimensions of 3D physical model.

Table 4 Stable values of characteristic performances of TE module.

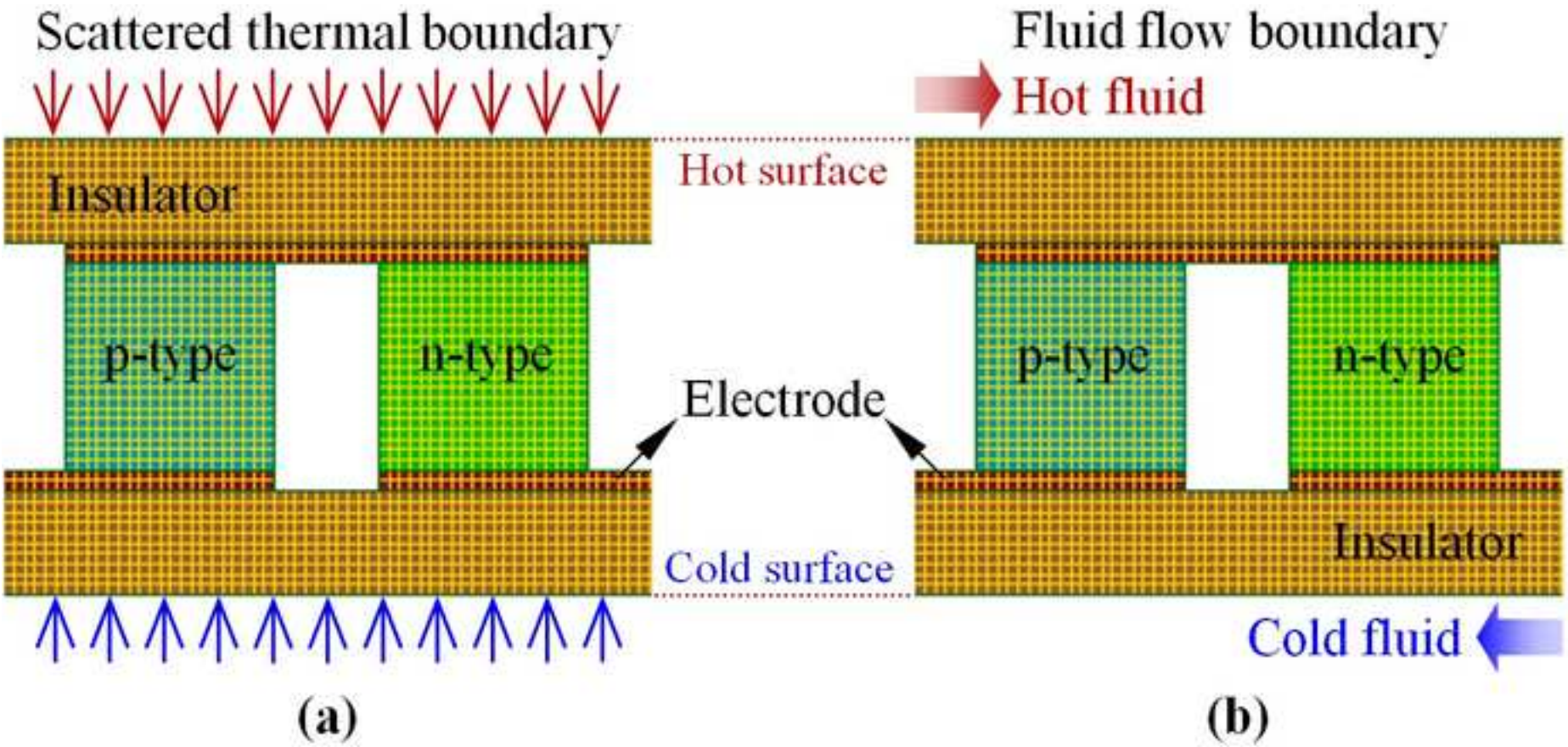

Figure_2

Click here to download Figure Figure_2.jpg

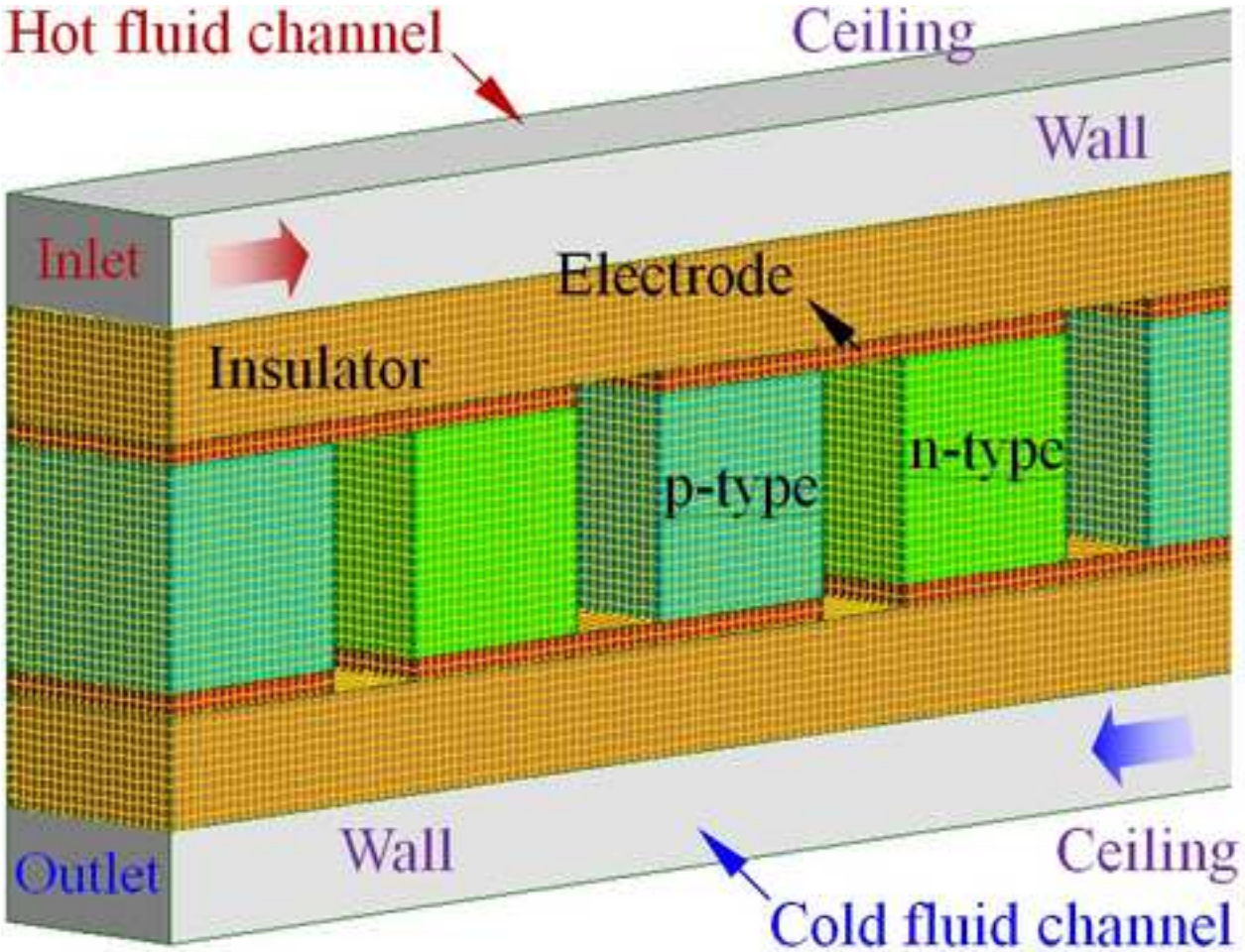

Figure_3_a

Click here to download Figure Figure_3_a.jpg

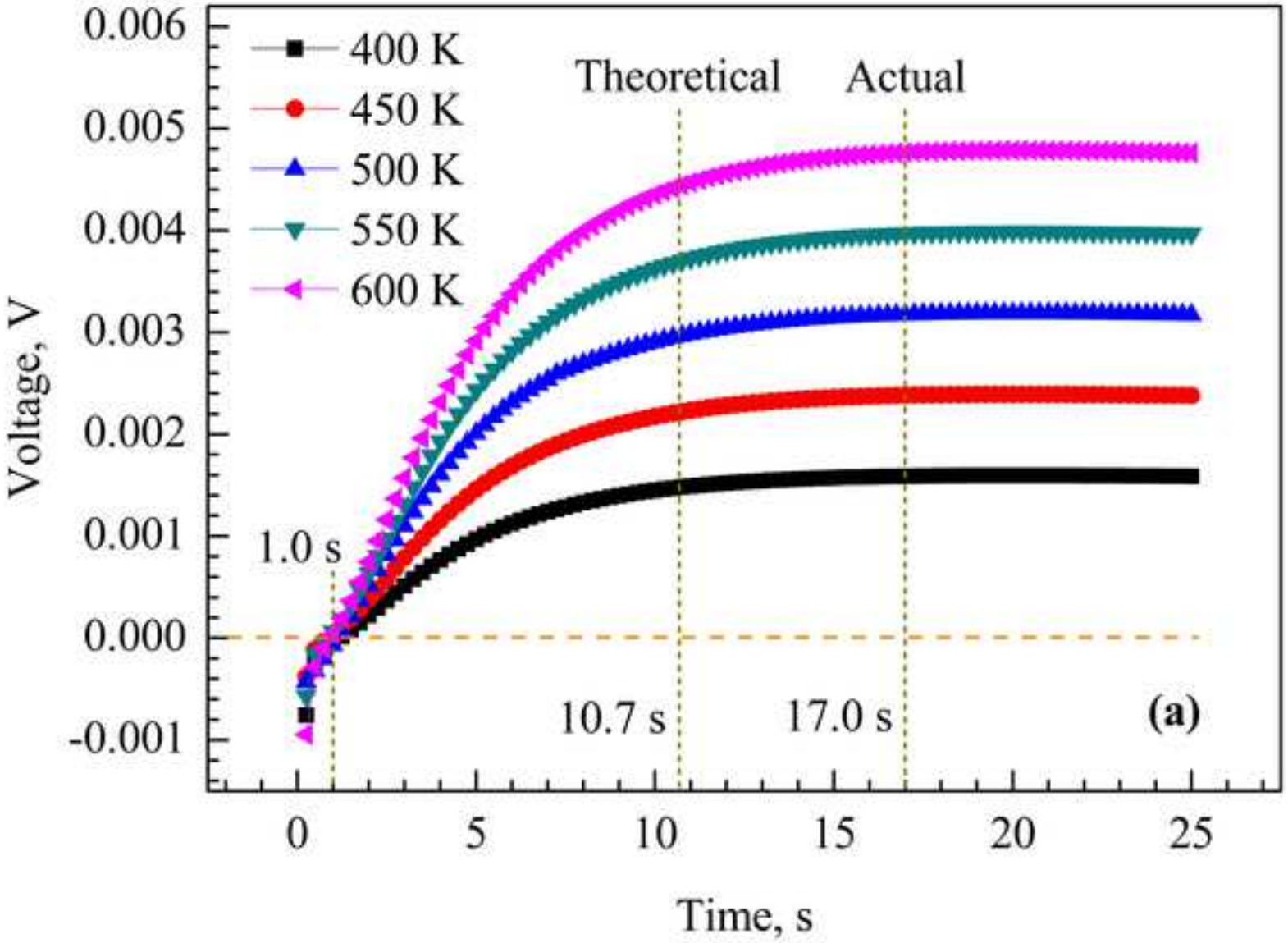

Figure_3_b

Click here to download Figure Figure_3_b.jpg

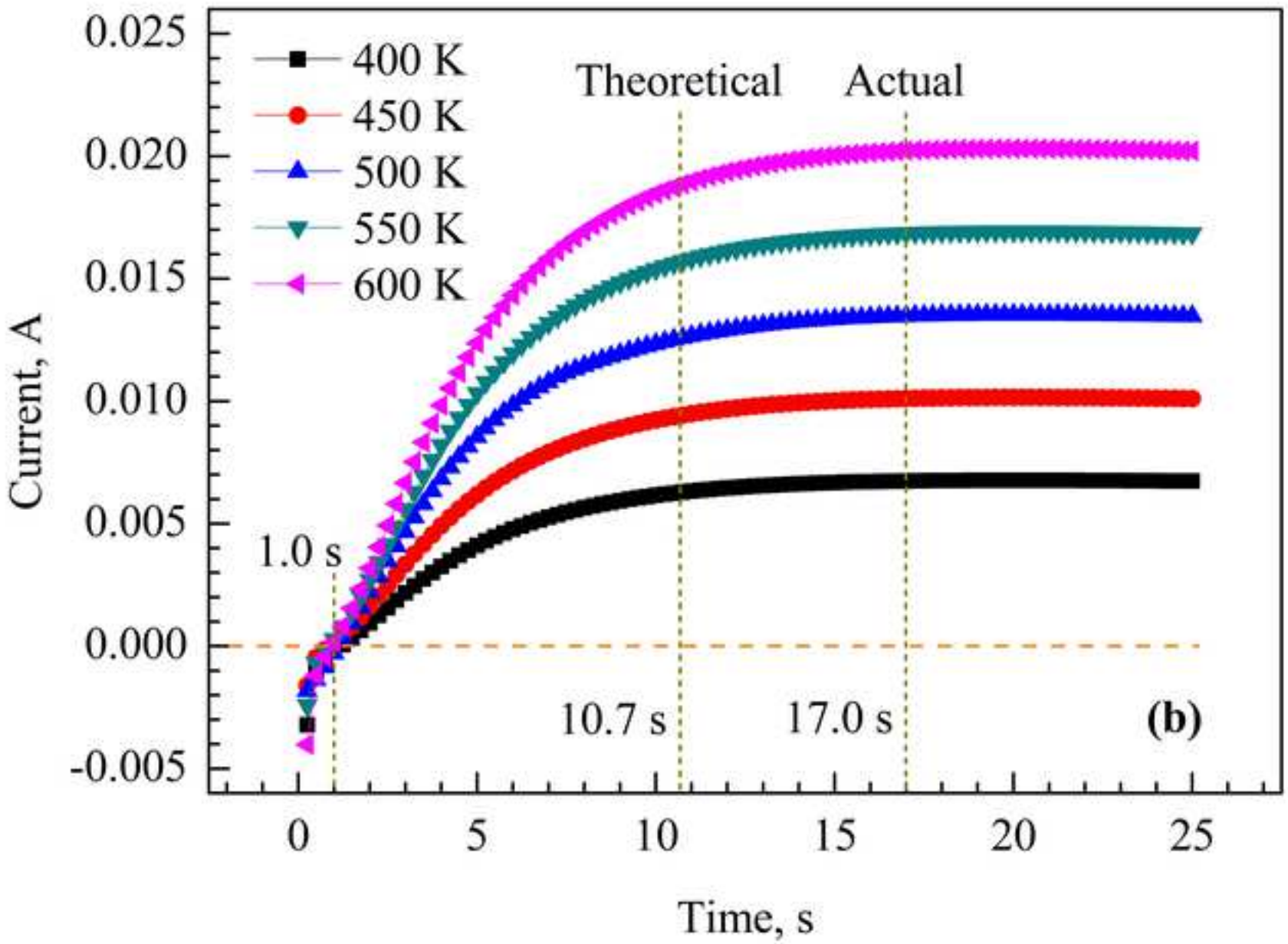

Figure_3_c

Click here to download Figure Figure_3_c.jpg

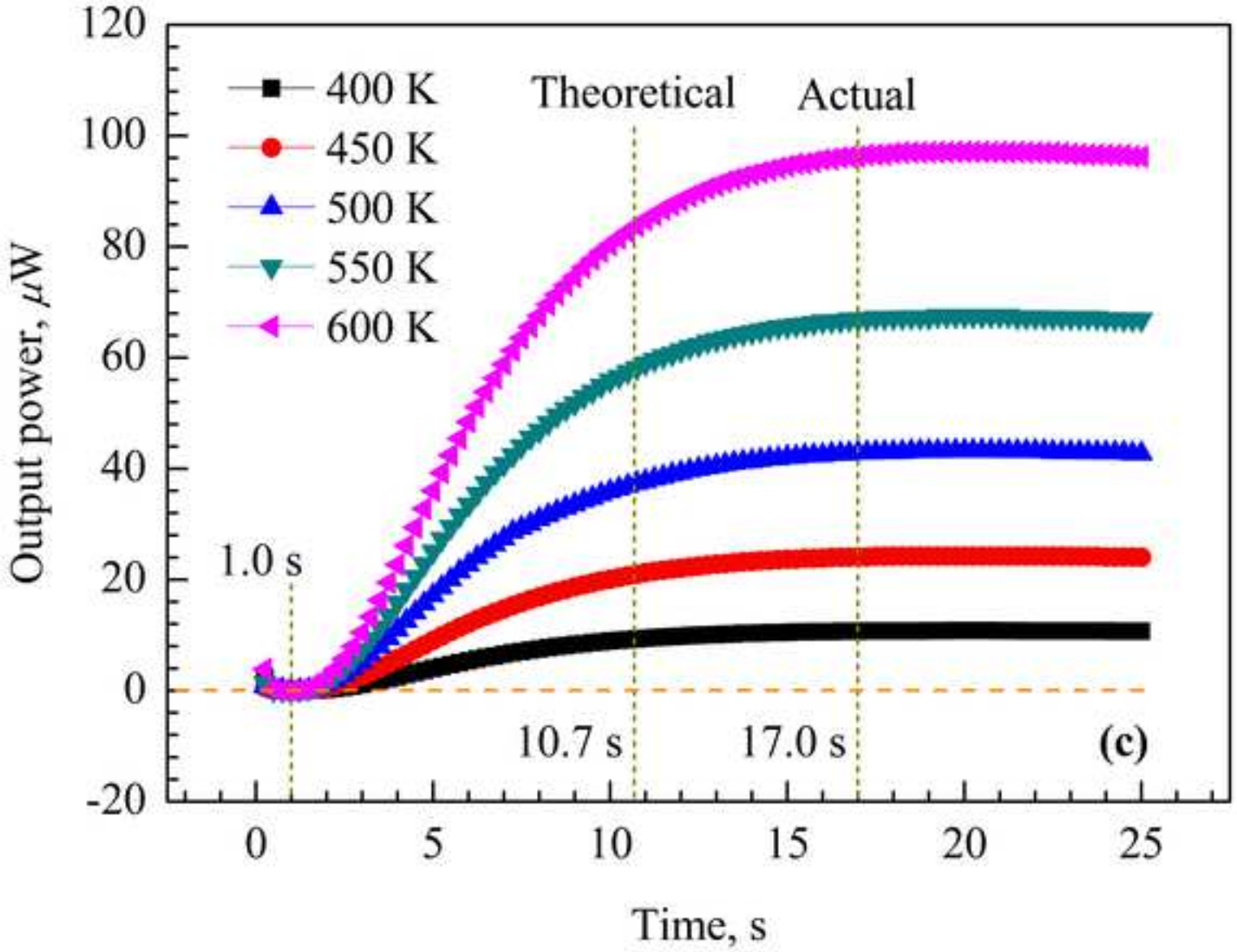

Figure_4

Click here to download Figure Figure_4.jpg

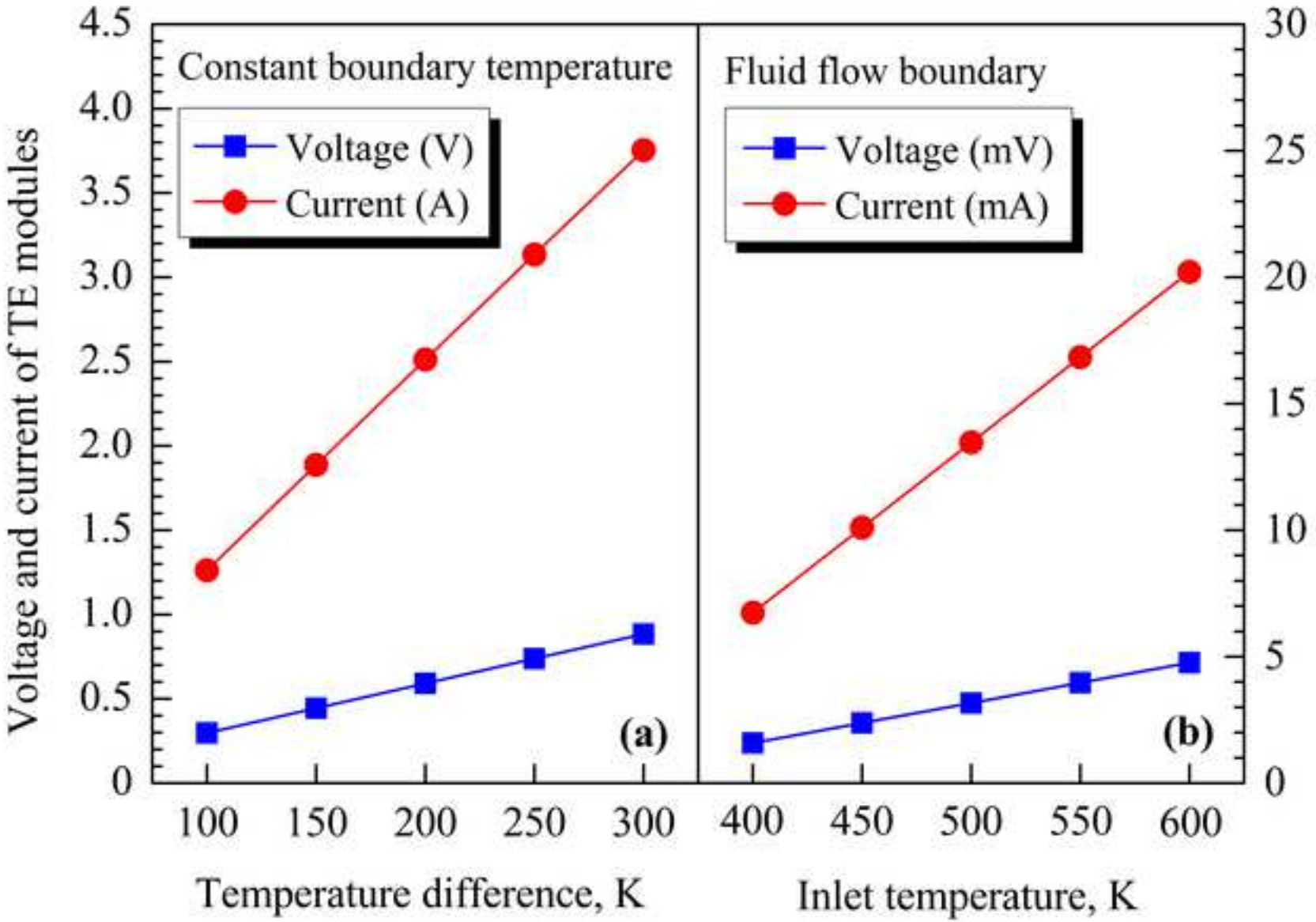

Figure_5

Click here to download Figure Figure_5.jpg

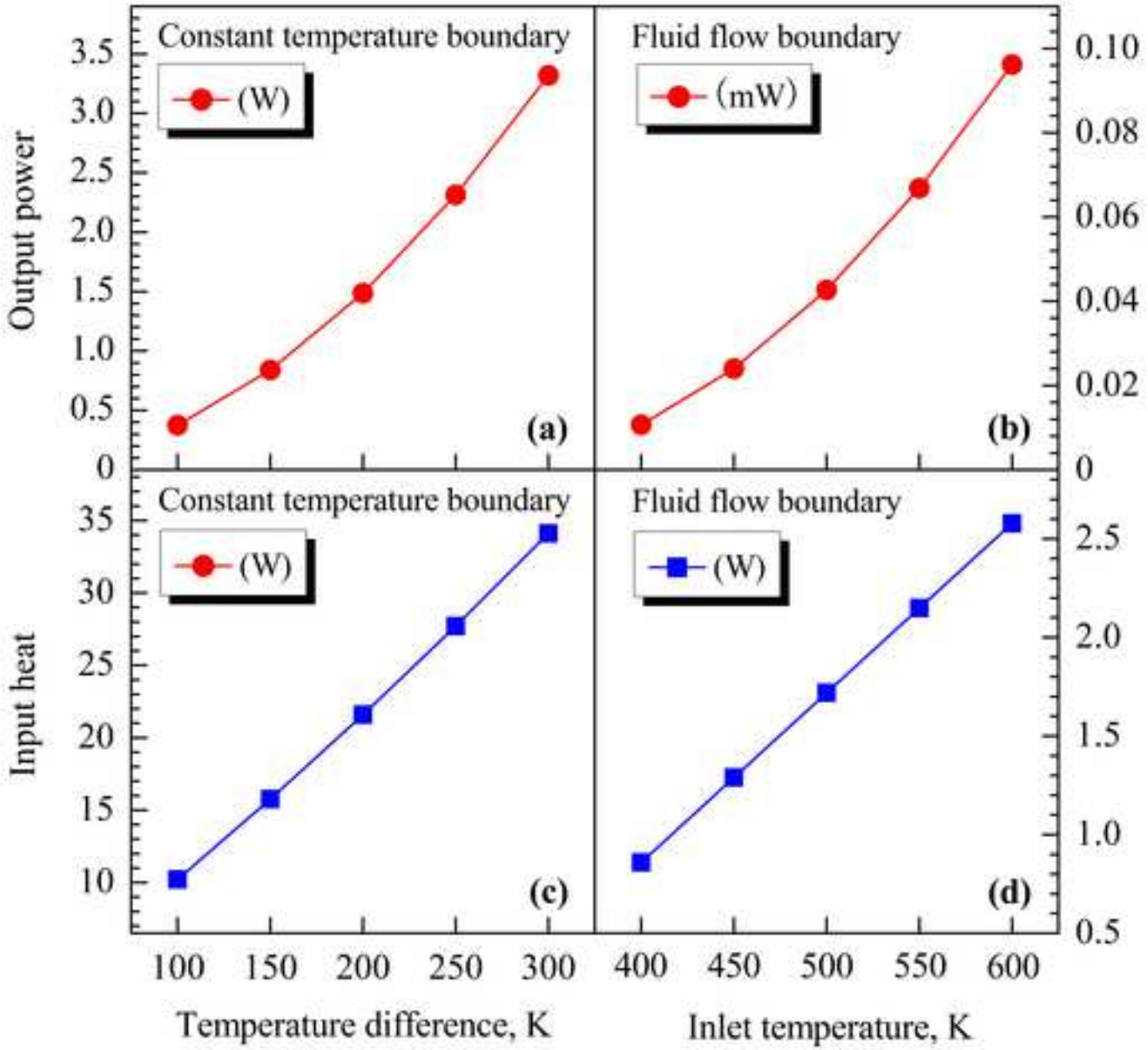

Figure_6

Click here to download Figure Figure_6.jpg

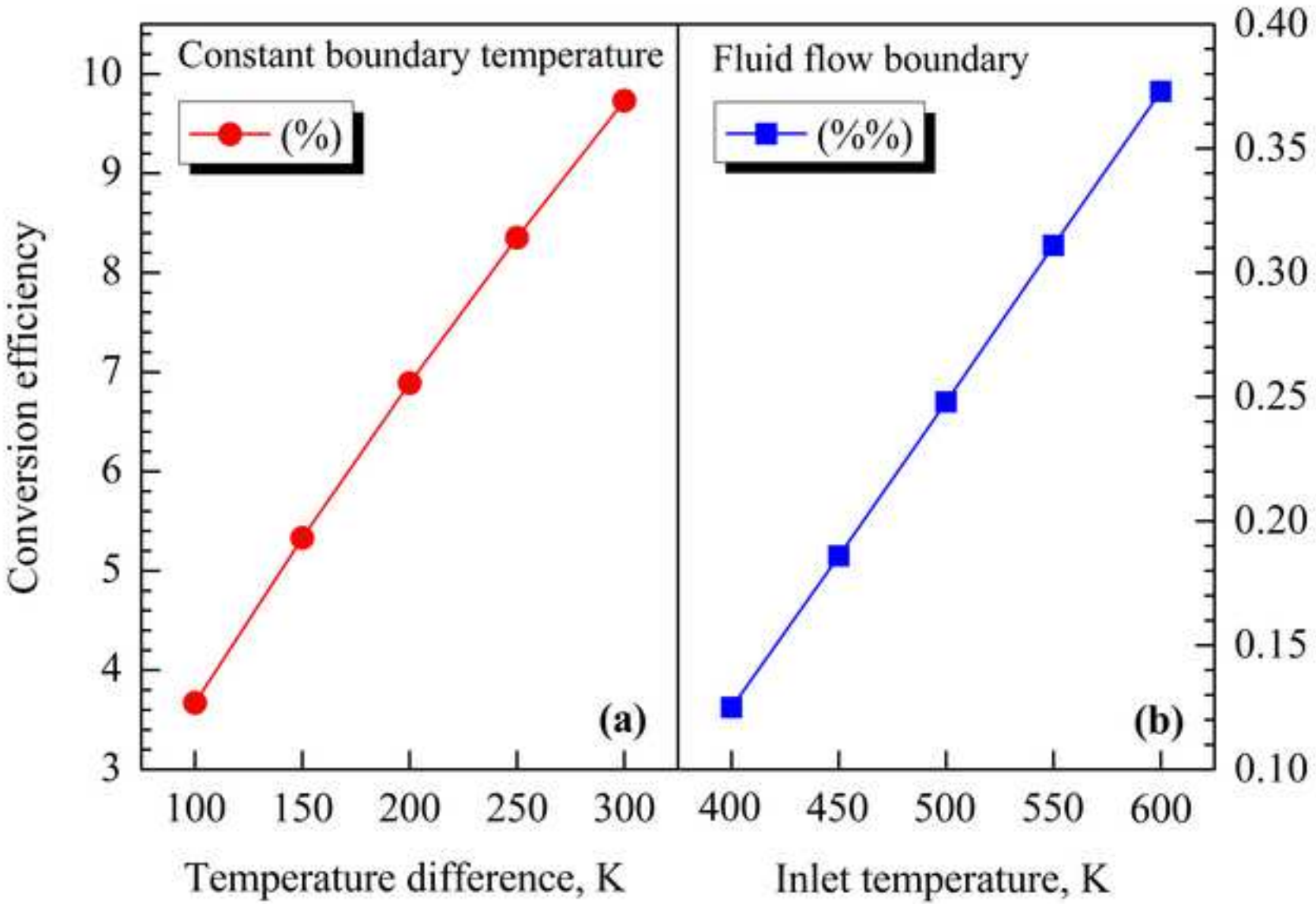

Figure_7

Click here to download Figure Figure_7.jpg

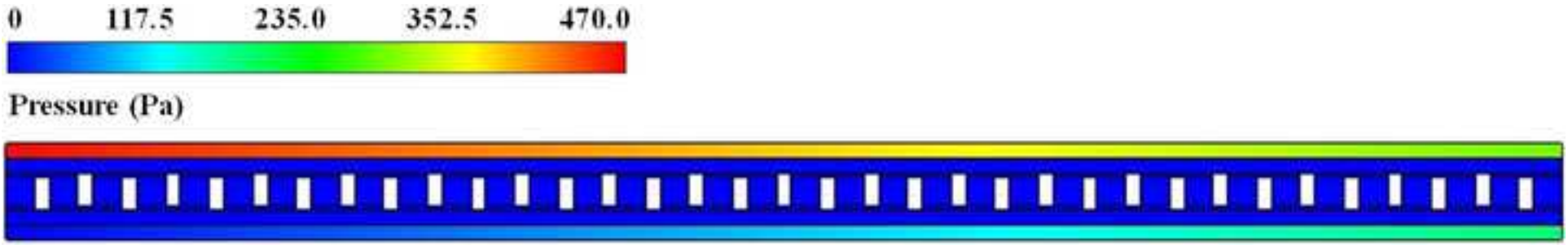

Figure_8

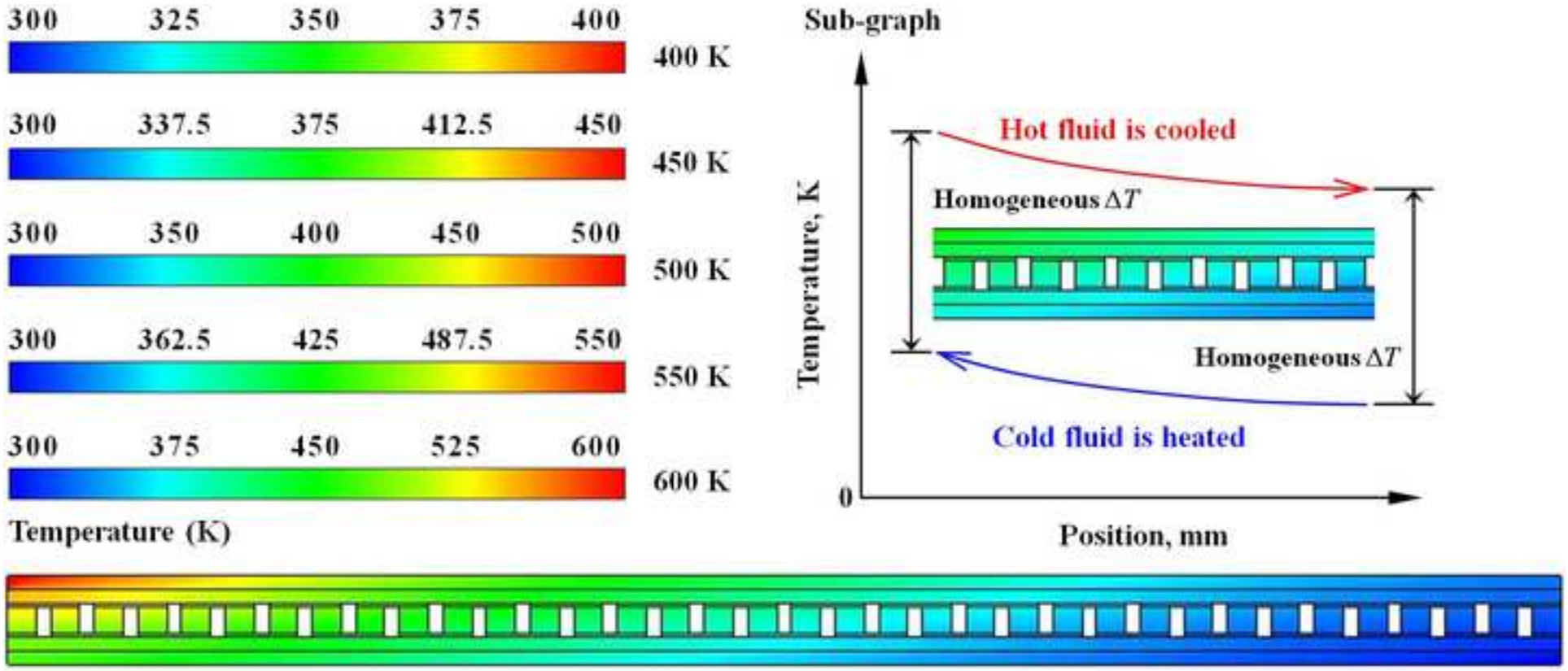

Figure_9

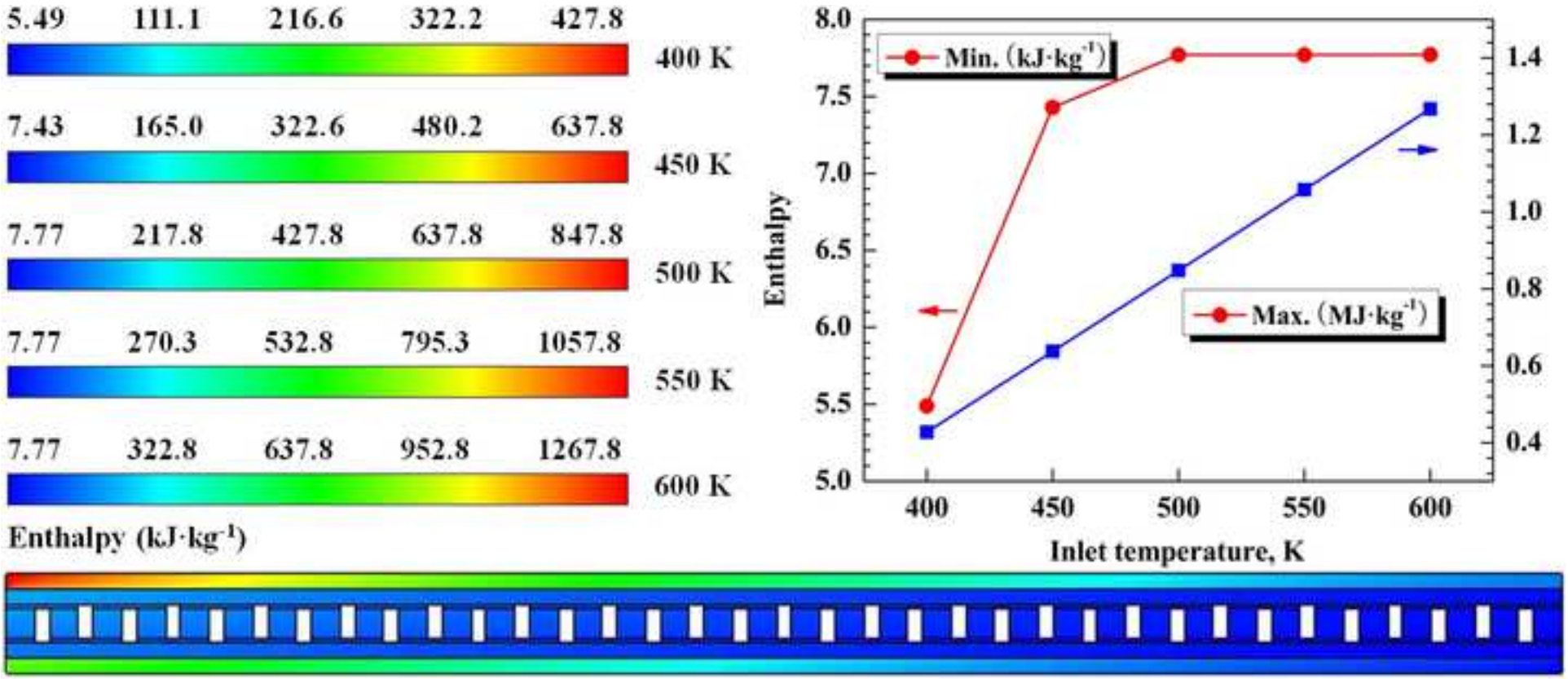

Figure_10

Click here to download Figure Figure_10.jpg

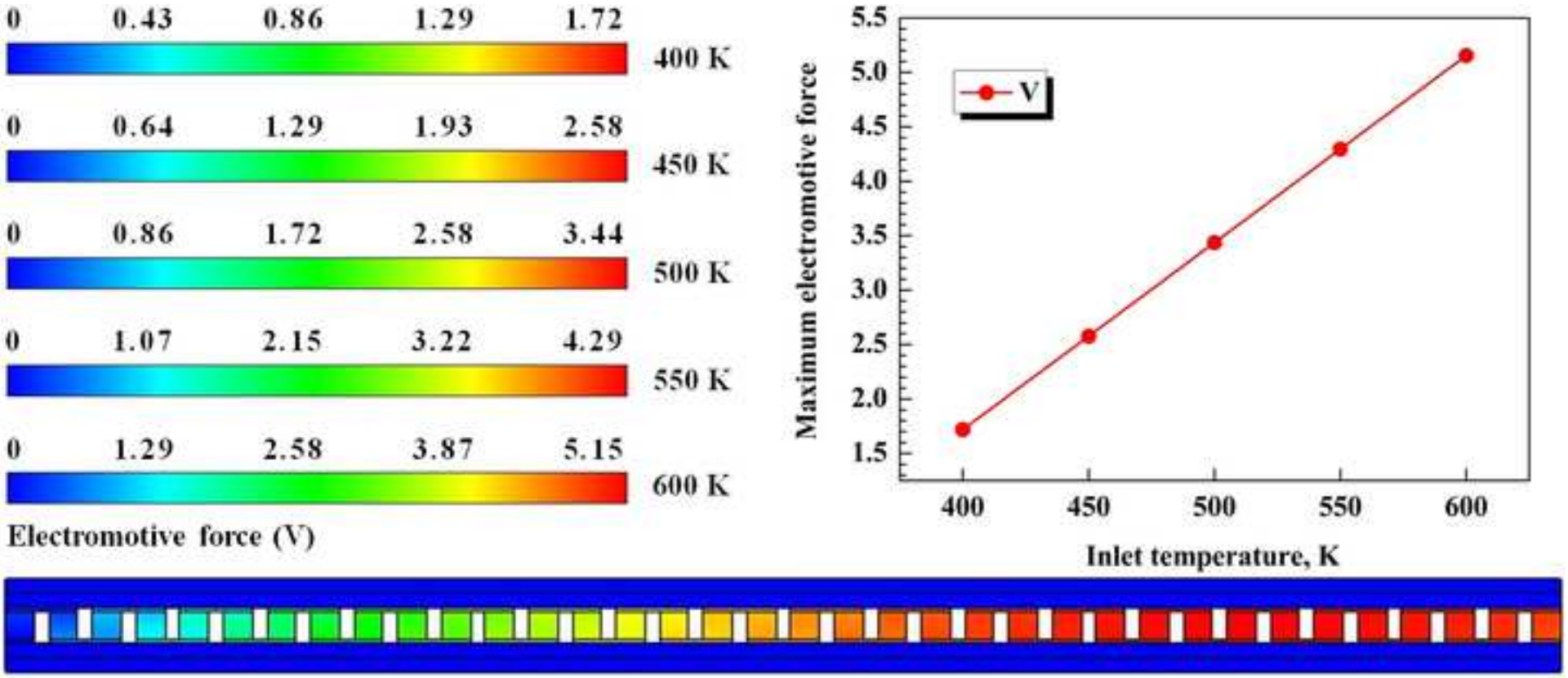

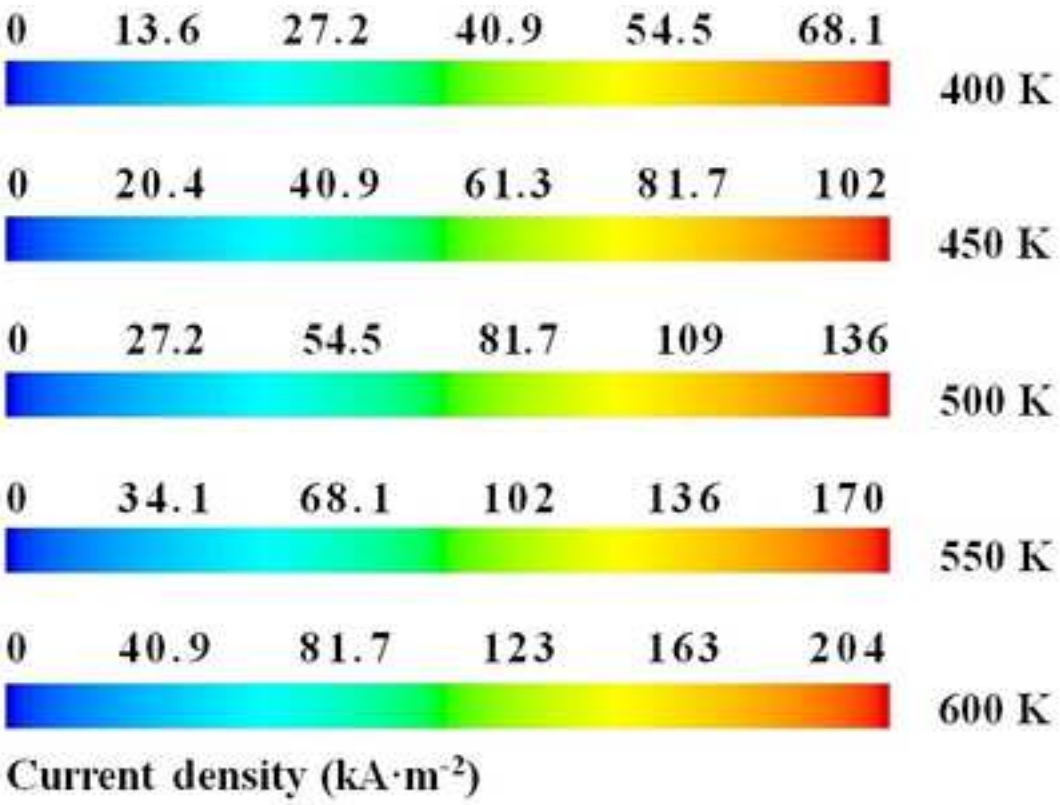

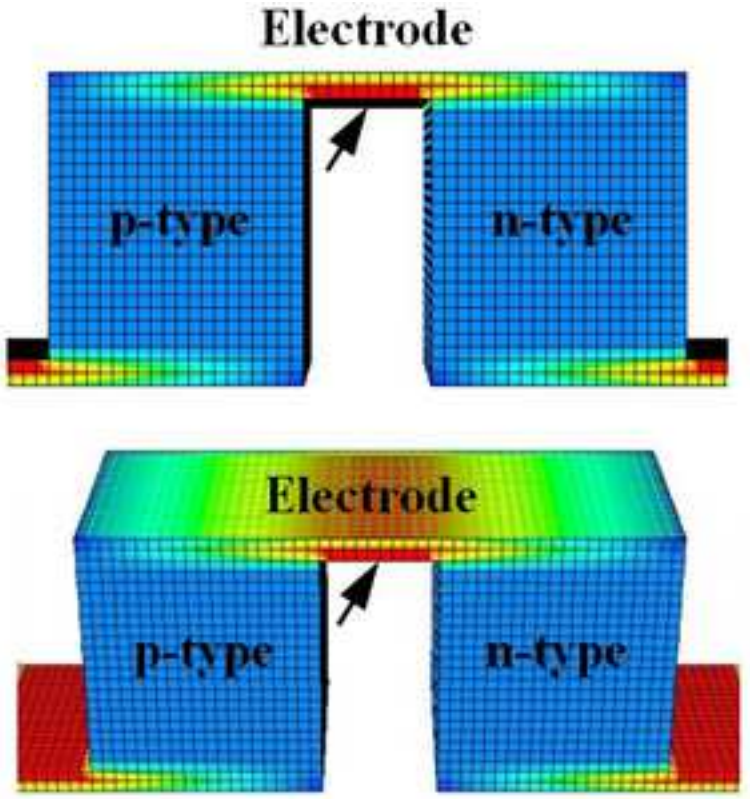

Figure_12

Click here to download Figure Figure_12.jpg

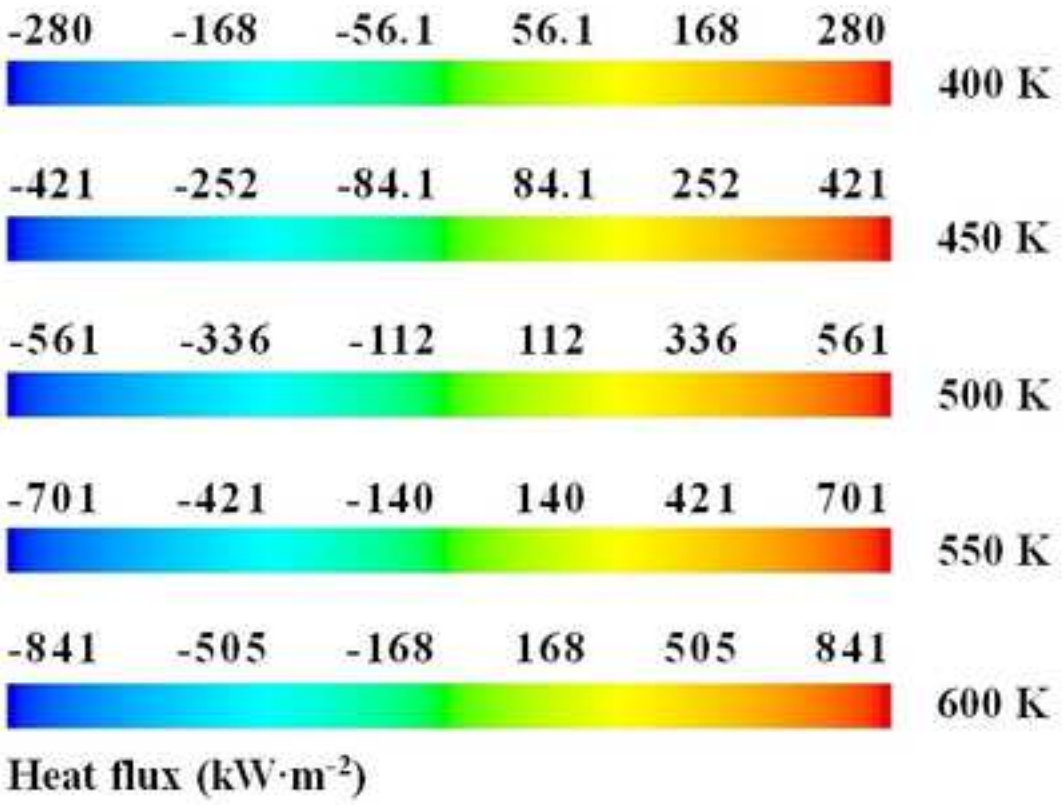

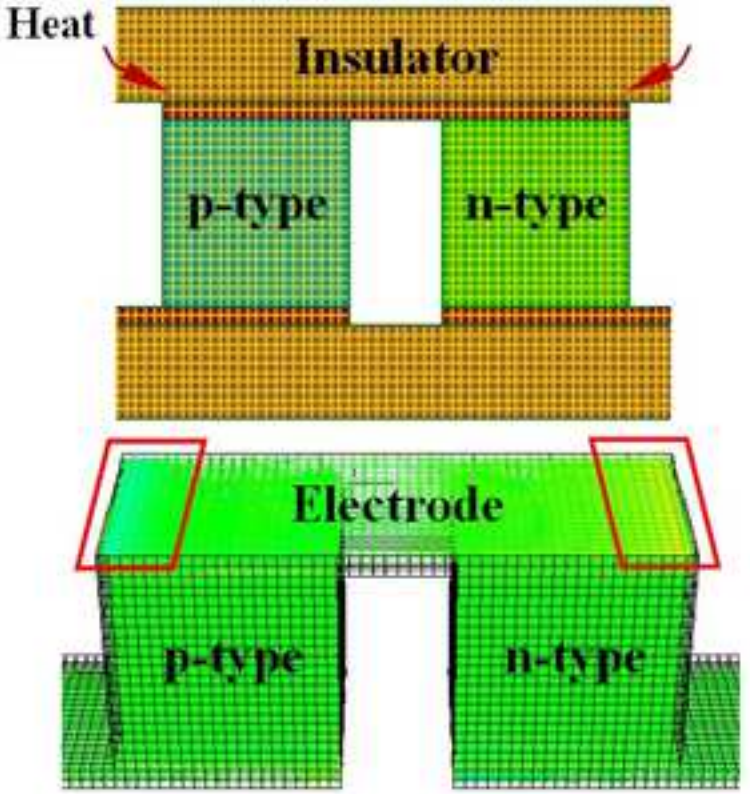

Table 1 Thermal and electric properties of materials [9, 10].

Materials	Seebeck coefficient ($\mu V \cdot K^{-1}$)	Electric resistivity ($10^{-6} \cdot \Omega \cdot m$)	Thermal conductivity ($W \cdot m^{-1} \cdot K^{-1}$)
Bi_2Te_3 (p-type)	190	5.5	2.06
Bi_2Te_3 (n-type)	210	10.0	2.02
Cu (electrode)	1.83	0.0155	398
Al_2O_3 (insulator)			36

Table 2 Physical properties of water at ambient temperature.

Density ($kg \cdot m^{-3}$)	Specific heat ($kJ \cdot kg^{-1} \cdot K^{-1}$)	Viscosity ($10^{-5} \cdot Pa \cdot s$)	Thermal conductivity ($W \cdot m^{-1} \cdot K^{-1}$)
1000	4.18	100	0.6

Table 3 Geometric dimensions of 3D physical model.

Elements (p-type and n-type)			Electrodes		Insulators		Channels	
Area (mm^2)	Leg height (mm)	Width (mm)	Thickness (mm)	Width (mm)	Thickness (mm)	Width (mm)	Wall (mm)	Ceiling (mm)
1.0	1.0	1.0	0.1	1.0	0.5	1.0	0.5	1.0

Table 4 Stable values of characteristic performances of TE module.

Inlet temperature	Voltage (mV)		Current (mA)		Output power (mW)	
(K)	Value	Increment	Value	Increment	Value	Increment
400	1.59		6.74		10.72	
450	2.38		10.1		24.04	13.32
500	3.17	0.79	13.47	3.37	42.7	18.66
550	3.97		16.84		66.85	24.15
600	4.76		20.21		96.2	29.35